Journal of Materials Chemistry A

REVIEW

View Article Online
View Journal | View Issue

Cite this: J. Mater. Chem. A, 2024, 12, 14229

Infrared spectroscopy for understanding the structure of Nafion and its associated properties

Tanya Agarwal, [ab] Ajay K. Prasad,[b] Suresh G. Advani, [b] Siddharth Komini Babu [a] and Rodney L. Borup *[a]

Significant effort has been invested previously to understand the effect of temperature and humidity on water uptake, water transport, structure, and proton conductivity of perfluorosulfonic acid (PFSA) ionomer membranes. One of the significant factors influencing the performance and durability of Nafion is its ability to retain and transport water. Water transport in Nafion is a strong function of sorption, ion exchange capacity, and transport properties of the membrane, which in turn, are functions of its structure and morphology. In addition to the operating conditions, pre-treatment conditions, additives, and the presence of cations significantly affect Nafion's morphology. Infrared spectroscopy (IR) is a powerful tool to gain insight into the properties of Nafion structure and properties. FTIR can monitor real-time changes in chemical interactions, molecular motions, and connectivity of ionic channels under varying operating conditions. FTIR has also been used to validate models developed to explain the dynamic behavior of polymer electrolyte membrane fuel cells. The potential of infrared spectroscopy to understand the impact of environmental changes on Nafion structure is immense but remains underutilized. This review provides a comprehensive summary of the assignment of vibrational modes of Nafion in various regions of the spectrum and sheds light on discrepancies concerning the allocation of vibrational modes to specific interactions.

Received 18th September 2023
Accepted 28th March 2024

DOI: 10.1039/d3ta05653h

rsc.li/materials-a

1 Introduction

Nafion is a perfluorosulfonic acid (PFSA) polymer developed by DuPont in 1966.[1] The cation transport properties of Nafion are central to its use in diverse applications. The biggest application for Nafion is in the chlor-alkali industry, but it also finds applications in fuel cells, electrolysis, catalysis, selective removal of various cations, batteries, sensors, and stimuli-responsive materials. Relevant to this review paper, Nafion is widely used as the polymer electrolyte membrane (PEM) in fuel cells and electrolyzers.

As shown in Fig. 1, Nafion consists of a polytetrafluoroethylene (PTFE) backbone with ionic side chains terminating in a sulfonic acid group. The hydrophobic PTFE backbone provides mechanical and chemical strength, while the sulfonic acid side chain is responsible for Nafion's proton transport properties. This combination of a hydrophobic backbone with a hydrophilic side chain results in a phase-separated morphology that is responsible for the unique transport properties of Nafion.[2] Other perfluorosulfonic acid polymers investigated in the literature include Aquivion,[3] Flemion,[4] Fumion,[5] Aciplex,[6] 3M perfluorosulfonimide (PFIA) membrane terminated in sulfonic acid like other PFSAs,[7] and PFSA from DOW chemicals.[6] The general structure of all these membranes is shown in Fig. 1, where m, n, x, and y vary depending on the supplier. PFSAs are usually characterized in terms of its equivalent weight (EW) and ion exchange capacity (IEC). EW is a measure of the concentration of sulfonic acid sites within the membrane, with higher EW indicating a lower degree of sulfonation. The presence of water results in the dissociation of sulfonic acid groups in the side chains, which enables proton transport. Water content in PFSA is usually described in terms of λ which is defined as the moles of water per mole of sulfonic

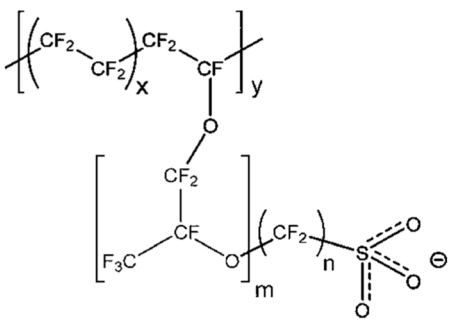

Fig. 1 Molecular structure of Nafion.

[a]MPA-11: Materials Synthesis & Integrated Devices, Los Alamos National Laboratory, Los Alamos, New Mexico 87545, USA. E-mail: borup@lanl.gov

[b]Center for Fuel Cell Research, Department of Mechanical Engineering, University of Delaware, Newark, Delaware 19716, USA

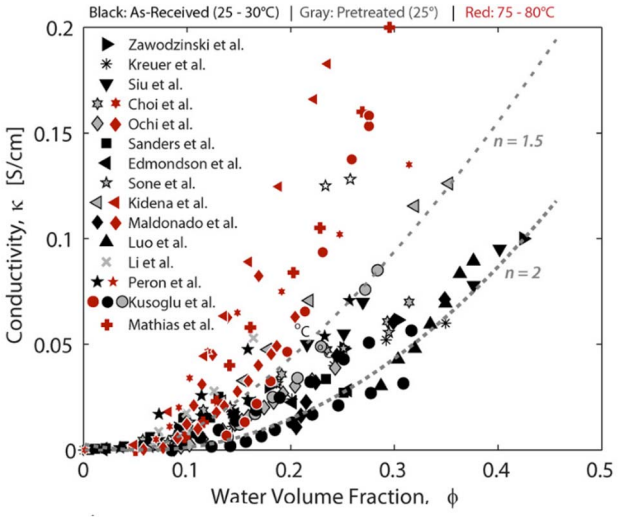

Fig. 2 Proton conductivity of PFSA as a function of water content.[9] Reproduced with permission from ACS Publications.

acid sites.[8] Under low water content and high temperatures, PFSA is practically non-conducting to protons[9] as shown in Fig. 2. Under high water content, the membrane becomes highly conducting to protons due to the dissociation of the sulfonic acid group.[9]

Nafion was the first PFSA discovered which is also why it has been a topic of intensive research for more than 40 years. The use of Fourier Transform Infrared Spectroscopy (FTIR) to investigate the properties of perfluorosulfonate ionomers dates to the 1980s when Lowry and Mauritz[10] used it to study the effects of hydration. Dynamic water sorption, Thermogravimetric Analysis (TGA), Differential Scanning Calorimetry (DSC), water uptake studies, and proton conductivity changes have been used in the literature to understand the dynamics of water sorption and structure–property relationships in PFSA, as well as to understand the degradation mechanisms as a function of changing environmental factors for PFSAs. Several other characterization tools that are periodically used for structural investigations of PFSA include X-ray Diffraction (XRD), Small Angle X-ray Diffraction (SAXS),[11,12] Wide Angle X-ray Diffraction (WAXS), Neutron Reflectometry (NR)[13,14] and Small Angle Neutron Scattering (SANS).[15] A less utilized yet more available technique for studying smaller local structural changes is FTIR.

FTIR is a powerful tool to gain fundamental insights into the molecular level interactions within PFSAs in a non-destructive manner and to relate them to its macroscale properties. FTIR can deduce local changes in the chemical environment of PFSA from changes in the vibrational frequency of the various bonds. Commonly observed vibrational modes in molecules is shown in Fig. 3. FTIR operates by measuring the interaction between matter and an applied electromagnetic field in the infrared region. When infrared radiation is incident on a sample, the incident energy is absorbed if the frequency of the photons coincides with the vibrational energy level of the molecule. When the environment around the molecule is changed, the vibrational frequencies of the various bonds change and so does the energy of the photon absorbed. These changes are recorded in the form of an FTIR spectra. A shift in the vibrational modes, changes in intensities, or the appearance and disappearance of peaks are accurate indicators of changes at the molecular scale in the vicinity of specific groups. Hence, FTIR represents a sensitive technique for measuring molecular level changes. Some of the common vibrational modes observed for a molecule are shown in Fig. 3.

The commonly used sampling methods for vibrational spectroscopy includes Attenuated Total Reflection (ATR) and Transmission Spectroscopy. In ATR, light passes through a crystal surface and interacts with the crystal sample interface at 45° angle of incidence. Typical crystals used for ATR include Zinc Selenide (ZnSe), diamond and germanium. In transmission spectroscopy, the light passes directly through the sample.

The FTIR technique provides advantages such as ease of use and universality of applications. It is powerful because it offers unparalleled measurement speed with the ability to measure relevant frequencies within seconds. The short measurement time ensures that the sample measurement can be repeated to reduce noise in a matter of minutes. It also employs very

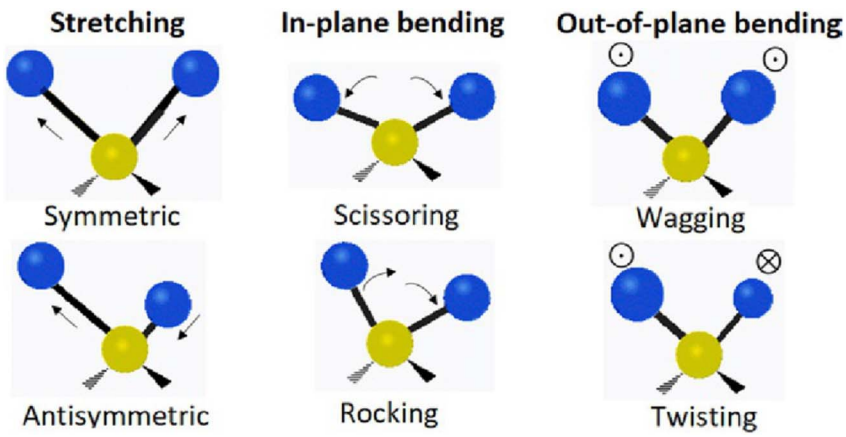

Fig. 3 Common vibrational modes observed.[16] Reproduced with permission from Elsevier.

sensitive detectors with high optical throughput. FTIR is a self-calibrating instrument containing few moving parts which minimizes mechanical breakdown and errors induced by human intervention. It can measure a variety of samples and detect even the smallest amount of contamination which makes it a valuable tool.[17]

To fully utilize the potential of FTIR, it is critical to precisely assign the vibrational modes to specific interactions. Changes in those interactions can then be correlated to changes in the macroscale properties.[3] FTIR spectroscopy of a system like PFSA is, however, not easy. FTIR of protonated species is complicated because of the overlapping presence of various peaks corresponding to different functional groups and vibrational states.[18] This makes the study of hydrated Nafion a challenge leading to several unanswered questions and conflicting findings.[19,20] This is also the reason that most of the work on Nafion is addressed towards lower wavenumber region, below 2000 cm^{-1} of the spectrum. Understanding the structure of Nafion has helped in the design of other types of membranes catering to various applications. It has also resulted in the development of new analytical techniques. Therefore, PFSA can continue to offer new possibilities when its chemistry is more completely understood.

2 Previous reviews

Several excellent reviews have been published on the structure–property relationship of Nafion. Mauritz and Moore[21] published a comprehensive review aimed at understanding the morphology of Nafion, the structure of its ionic clusters, and how SAXS, WAXS, and other characterization data come together to support the various models suggested in the literature. These authors found no model that could predict the behavior of Nafion in various environments and attributed it to the challenging nature of its structure. A recent review discussed advanced methods for understanding molecular ordering and features of conducting channels in Nafion membranes.[22] Hickner *et al.*[23] highlighted the problems associated with using different ionomers in the electrodes while using Nafion as the electrolyte membrane, and also comprehensively discussed past work aimed at understanding the properties of Nafion. Duncan *et al.*[24] published an elaborate review on the application of Nafion in ionic polymer transducers (IPT) and how the systematic investigation of its properties has helped design new polymers to improve IPT performance over time. Kusoglu *et al.*[9] compiled an extensive dataset from various studies to understand the structure–property correlation of Nafion. In a recent review, Choi *et al.*[25] highlighted the influence of structure on the crystalline domains of PFSAs and the influence of the nanostructure on PFSA mechanical properties. Okonkwo *et al.*[26] comprehensively reviewed the degradation studies on Nafion. Yan *et al.*[27] examined the properties of Nafion thin films as opposed to membranes, and investigated aggregate structures in catalyst layers and film structure in detail.

This review collects and organizes the various FTIR investigations on Nafion to elucidate how this tool has helped to gain fundamental insights into Nafion as it exists today, unfold its complex structure, and explain the observed property changes with various environmental changes. It aims to stimulate the use of FTIR for additional investigations of Nafion. This review also aims to highlight the discrepancies between FTIR assignments of Nafion and how its resolution would further help in understanding PFSAs.

The review is organized as follows:

(1) We first examine how the understanding of vibrational modes of Nafion's sidechains has evolved over time. This includes determination of vibrational modes attributed to sulfonic acid groups in Section 3.1.1, ether group modes in Section 3.1.2, and C–S vibrational mode in Section 3.1.3. Vibrational modes under dry conditions for the side chain of Nafion is discussed are in Section 3.2. The effects of annealing and aging (Section 3.3) on Nafion's properties by examining changes in the Nafion sidechain vibrational modes are henceforth discussed in Section 3.3. We also evaluate the reasons for discrepancies in the assignment of vibrational modes to the sidechains in each section and identify areas that need further work. This section discusses side chain vibrational modes that have laid the foundation for explaining Nafion transport properties over time.

(2) We review the influence of cations on the vibrational modes of Nafion's sulfonic acid groups and water environment in Section 3.4. This section highlights the complex nature of Nafion environment as a function of changing molecular environment of Nafion.

(3) Section 4 discusses studies relating to the assignment of vibrational modes to the polymer backbone of Nafion.

(4) Studies relating to the vibrational modes of Nafion due to the presence of water are discussed in Section 5. This section highlights how FTIR alone could explain complex transport properties of Nafion by closely following vibrational modes of water as a function of environmental changes, in conjunction with the changes in side chain vibrational modes.

3 Ionic vibrational region

Nafion is interesting for various applications because of its proton transport properties. Accordingly, we first consider the ionic vibrational region associated with the proton transport properties of the membrane. This region consists of vibrational modes associated with the Nafion side chain. The vibrational modes in this region belong to the stretching, bending and wagging vibrations from C–F, C–O–C, C–S, and SO_3^-. The FTIR spectrum for as-received Nafion 212 under ambient conditions of 25 °C, 30% RH conditions is shown in Fig. 4, and the major vibrational modes observed for it along with their assignments are presented in Table 1. The region below 800 cm^{-1} consists of overlapped peaks from bending, and wagging modes of side chain functional groups and represents the fingerprint for a given polymer. Changes in the fingerprint region are indicative of changes in the structure of the polymer.

Single functional group assignments have caused a lot of confusion for decades and are still a topic of debate. For example, some groups[28,32] assigned the peak at 512 cm^{-1} to

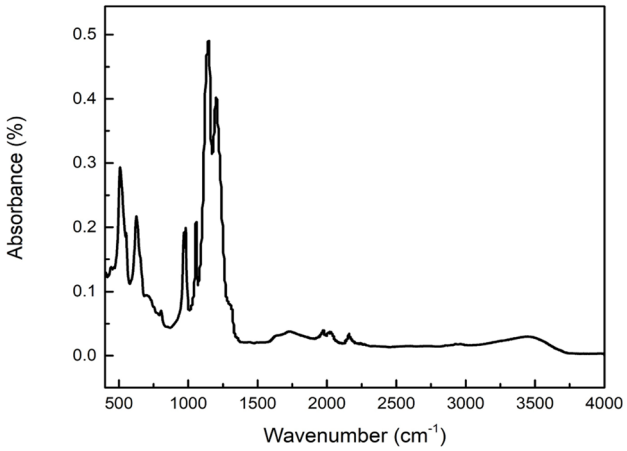

Fig. 4 FTIR spectra of Nafion 212 recorded at ambient conditions in our lab.

Table 1 Major vibrational modes of a Nafion side chain

Wavenumber (cm^{-1})	Assignment
513 [28]	Symmetric O–S–O stretching
553 [28]	Asymmetric C–F bending
629 [29]	CF_2 wagging
808 [30]	C–S stretching
970 [18]	C–O–C stretching
982 [31]	Asymmetric C–O–C stretching
1060 [2]	Symmetric SO_3^- stretching
1150 [29]	Asymmetric CF_2 stretching
1210 [30]	Symmetric CF_2 stretching
1315 [18]	Asymmetric SO_3^-stretching

asymmetric O–S–O stretching while others[29] assigned this peak to CF_2 rocking and wagging vibrations by comparing with the spectrum of polytetrafluoroethylene (PTFE) as shown in Fig. 5. The small peak observed at 731 cm^{-1} was assigned to C–C stretching by some groups[30] while others[29,33] assigned it to CF_2 symmetric stretching. The accurate assignment of peaks in the FTIR spectra to specific vibrational modes is non-trivial, and therefore, still a matter of investigation in the research community. These issues will be explored in the following subsections.

3.1 Assignment of vibrational modes to Nafion side chains

A typical spectrum for the Nafion sidechain vibrational region is as shown in Fig. 6. The first known FTIR spectrum for Nafion was recorded in 1976 by Lopez *et al.*[34] who observed three major peaks for the Na^+ form of Nafion. OH stretching of water was observed at 3530 cm^{-1}, C–F stretching at 2350 cm^{-1}, and water scissoring at 1630 cm^{-1}. The region between 500 cm^{-1} and 1350 cm^{-1} was opaque and could not be recorded. This problem was solved by Heitnerwirguin[32] by collecting reflectance spectra along with the absorbance spectra for Nafion. Assignments of vibrational modes for the Nafion-like system could be simplified by comparing its spectra with the spectra of simpler

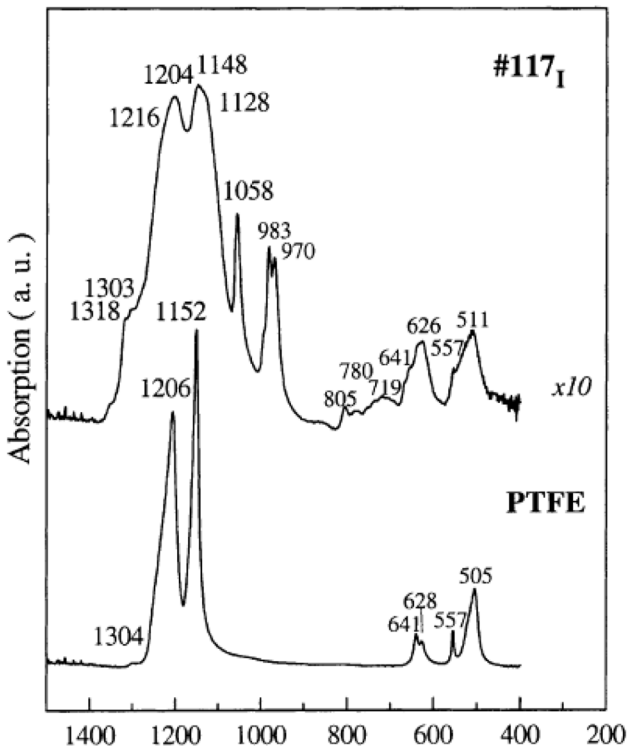

Fig. 5 Vibrational modes of Nafion 117 compared to PTFE vibrational modes.[29] Reproduced with permission from Elsevier.

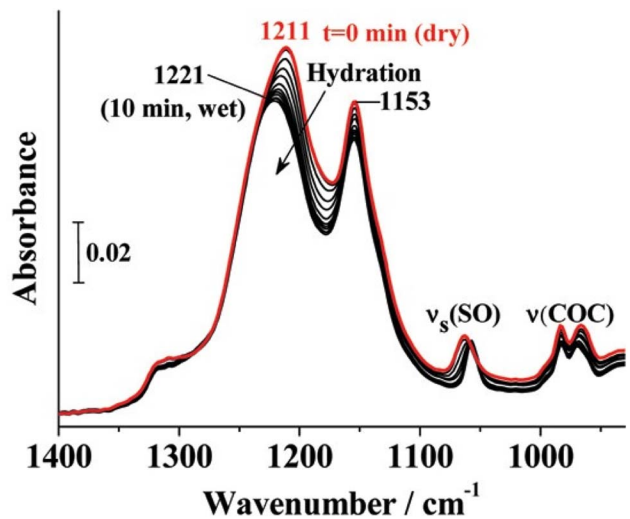

Fig. 6 Ionic vibrational region of Nafion.[35] Reproduced with permission from ACS Publications.

molecules containing the target functional group. Therefore, sulfonic acid group assignments for Nafion were made by comparing with the FTIR spectra of polystyrene sulfonic acid.[32] Similarly, C–O–C assignments were made by comparing with the spectra of polyoxymethylene,[32] and vibrational mode assignments of the Nafion backbone were made by comparing with the FTIR spectra of PTFE as shown in Fig. 5.

3.1.1 Sulfonic acid vibrational modes. Buzzoni *et al.*[18] studied the FTIR and Raman spectra of H_2SO_4 and CF_3SO_3H

(triflic acid), because their acidic character is analogous to Nafion. Comparing the peak assignments for these acids with those of Nafion can help resolve its spectrum. They found that the spectra for aqueous concentrated acids were different from those of pure acids, likely resulting from the transfer of protons to the water species. Concentrated $CF_3SO_3^-$ shows a strong absorption at 1040 cm^{-1}, HSO_4^- at 982 cm^{-1}, and SO_4^{2-} at 1050 cm^{-1}. 1060 cm^{-1} was therefore assigned to SO_3^- stretching in Nafion. Later, Danilczuk *et al.*[19] compared the FTIR spectrum of Nafion with Aquivion,[3] perfluoroimide acid (PFIA) made by 3M,[7] and other PFSA[6] polymers with sulfonic acid side chains like Nafion. They claimed 1060 cm^{-1} as the SO_3^- stretching mode after comparing the calculated assignments with the experimental results in agreement with Buzzoni *et al.*[18] Density Functional Theory (DFT) calculations performed using X3LYP exchange correlation functional taking $\lambda = 3$ show that 1060 cm^{-1} is dominated by the asymmetric stretching of the side chain ether group coupled to SO_3^- symmetric stretching in agreement with findings of other groups.[36,37] A similar result was obtained with DFT calculations when using the B3LYP exchange–correlation functional.[38] Loupe *et al.*[39] found 1060 cm^{-1} to be dominated by the C–O–C mode based on their DFT calculations for $\lambda = 4$. These findings suggest that 1060 cm^{-1} mode is not a single functional mode corresponding to $CF_3SO_3^-$ as initially speculated but is rather a group mode of ether stretching and sulfonic acid stretching mode.

Additional peaks are observed for Nafion in a dehydrated state. Two vibrational modes at 1420 cm^{-1} and 910 cm^{-1} are observed along with the absence of peak at 1060 cm^{-1}. These modes were resolved by comparing Nafion spectra to that of undissociated CF_3SO_3H. 1420 cm^{-1} was assigned to S=O stretching in Nafion and 910 cm^{-1} to S–OH stretching.[18] Two additional modes observed at 1150 cm^{-1} and 1200 cm^{-1} were ascribed to the SO_3^- asymmetric stretching by comparing Nafion with the spectrum of Perfluoro(2-ethoxyethane)sulfonic acid (PES) where these modes are observed at 1134 cm^{-1} and 1289 cm^{-1}. SO_3^- is a symmetric structure and shows a doubly degenerate asymmetric stretching mode. But the strong polarization of the hydronium ion could disturb this symmetry and result in a split peak as was observed at 1150 cm^{-1} and 1200 cm^{-1} in Nafion.[20,40] The asymmetric stretching peak of sulfonic acid at 1150 cm^{-1} was found to be a strong function of hydration.[20] For a partially hydrated membrane, this peak was spread over 1000–1100 cm^{-1}, blue shifting (increase in wavenumber) by 40–60 cm^{-1} with increasing hydration.[20]

3.1.2 Vibrational modes of the C–O–C group. The modes observed at 970 cm^{-1} and 980 cm^{-1} in the Nafion spectrum were assigned to C–O–C stretching.[32] The peak observed in Nafion at 980 cm^{-1} was not observed for Aquivion. Aquivion lacks a C–O–C side group, which supports the assignment of 980 cm^{-1} mode in Nafion to the C–O–C backbone group.[19] Aquivion shows a peak at 970 cm^{-1} and it has a C–O–C group closer to the $-SO_3H$ group, which supports the assignment of 970 cm^{-1} to the C–O–C side chain group of Nafion.[19] Two model compounds, PFMHSA, and PFEESA shown in Fig. 7 were investigated by FTIR which help understand mode assignments. PFEESA lacks the backbone C–O–C group and it also did not show the peak at 980 cm^{-1} which further supports these assignments.[19] This was further confirmed by the FTIR recorded for the 3M membrane which also lacks a C–O–C group close to its sidechain, and therefore did not show any mode at 970 cm^{-1}.[39]

Webber *et al.*[36] claimed from their DFT calculations performed using X3LYP functional for $\lambda = 0$ to 10, that the groups at 983 cm^{-1} and 970 cm^{-1} were dominated by $-SO_3^-$ symmetric stretching coupled to the ether group mode. Okamoto *et al.*[38] also found from their DFT calculations that the experimentally observed peak at 980 cm^{-1} is dominated by symmetric vibrations of $-SO_3^-$ in agreement with Webber *et al.*[36] Loupe *et al.*[39] used DFT calculations using X3LYP functional and molecular dynamic calculations performed using LAMMPS for $\lambda = 0$ to 20, and found that the 970 cm^{-1} mode is also dominated by the –

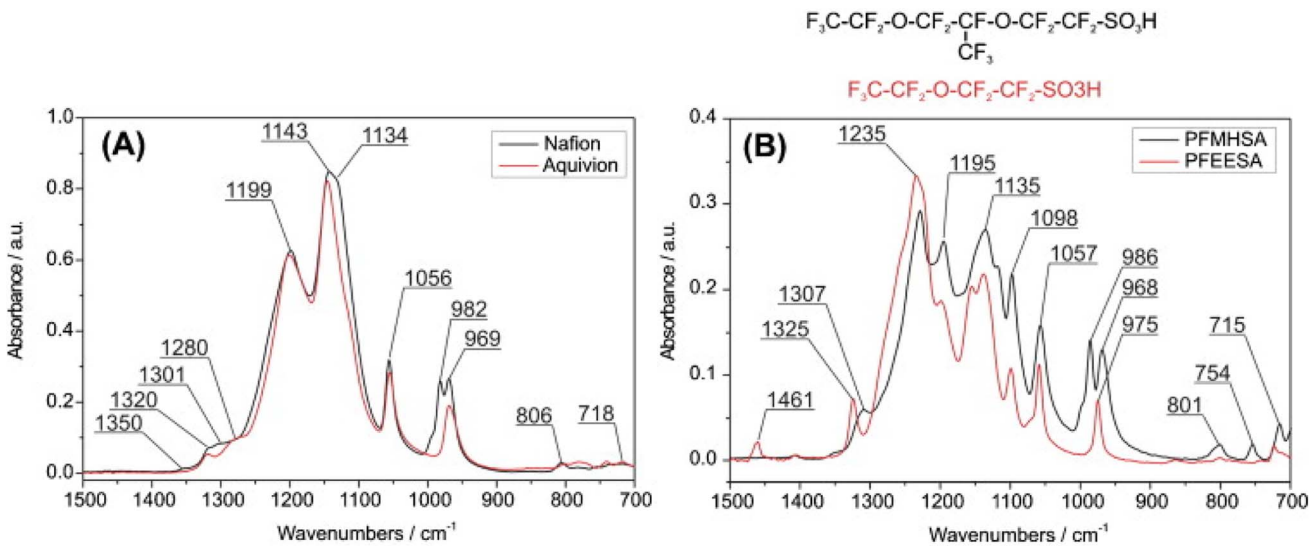

Fig. 7 (a) Spectra of Nafion compared to Aquivion (A) and other model compounds (B).[19] Reproduced with permission from Elsevier.

$CF_3SO_3^-$ stretching mode. In marked contrast to all the above studies, Danilczuk *et al.*[19] calculated C–O–C stretching modes to be in the 800 cm^{-1} region suggesting none of the modes in the 900–1000 cm^{-1} could come from the C–O–C mode. They claimed this based on the investigation of the model compounds and correlating the FTIR of model compounds to Nafion and Aquivion. They assigned 980 cm^{-1} to the stretching mode of $-CF_2$ groups in the side chain in agreement with Ferrari *et al.*[41,42] who assigned this mode to the stretching of –CF in the ($-CF_2-CF(R)-CF_3-$) groups of the sidechains that is absent in Aquivion.

The above studies suggest that 980 cm^{-1} and 970 cm^{-1} modes have contributions from –C–O–C stretching mode, C–S stretching mode, $-SO_3^-$ symmetric stretching mode and possibly C–F stretching modes that are strongly coupled to each other. Different modes could dominate at different hydration numbers and measurement conditions which could explain the discrepancy observed between the studies.

Another peak at 910 cm^{-1} is observed in the vibrational spectra of Nafion. This peak at 910 cm^{-1} was assigned to $-SO_3H$ symmetric stretching with C–O–C symmetric stretching as the secondary contributor.[39] The modes at 910 cm^{-1}, and 970 cm^{-1}, were found to be a strong function of hydration with C_1 (single functional group mode) dominating below $\lambda = 3$ and C_{3v} (three-fold symmetry) dominating above it.[39] The 980 cm^{-1} mode was not found to change much with hydration.[36] This indicates that the 980 cm^{-1} mode might not be dominated by $-SO_3^-$ symmetric stretching as calculated by Webber *et al.*[36] and others.[38] 980 cm^{-1} assignment to C–O–C stretching mode in the backbone or to the –CF stretching mode of the Nafion side chain follows the experimental observation that this mode is independent of hydration. However, further studies are needed to validate these findings. The peak at 970 cm^{-1} is likely a group mode of –C–O–C stretching and $-SO_3^-$ stretching, with the dominating mode being a function of hydration. Further experimental studies could help validate these assignments further.

3.1.3 Vibrational modes of the C–S group. DFT calculations for dissociated PES in the gas phase showed 967 cm^{-1} as the C–S symmetric stretching mode. This mode shifted to 952 cm^{-1} for undissociated PES.[20] The C–S stretching mode for Nafion was calculated at 974 cm^{-1} for the undissociated form and at 1019 cm^{-1} for the dissociated form[20] Etheve *et al.*[43] assigned the peak at 798 cm^{-1} to the C–S mode in agreement with Lage *et al.*[30] Danilczuk *et al.*[19] calculated that the C–O–C stretching mode should be observed in the 800 cm^{-1} vibrational region while other authors believe that 970 cm^{-1} is dominated by stretching modes of –C–O–C and $-SO_3^-$ as discussed in the previous section. Aquino *et al.*[40] calculated that the C–S mode has a main peak at 1066 cm^{-1} with side modes at 897 cm^{-1} and 1180 cm^{-1} for Nafion in sodium form. However, the peak at 1066 cm^{-1} is ascribed to the group mode of SO_3^- and C–O–C stretching as mentioned in the previous section.[19,39]

Since C–S vibrations are strongly coupled to the vibrational modes of C–O–C and SO_3^-, their vibrational modes span the range of 800–1300 cm^{-1}.[40] Various groups have tried to decouple –C–S stretching mode from the ether and sulfonic acid stretching modes in the side chain, and assign the observed peaks to a single vibrational mode which is a reason for controversies in the assignment of C–S modes. DFT calculations also vary widely in terms of the hydration level and the solvation model used for calculations. Peak assignment of 800 cm^{-1} mode remains unresolved and no clear agreement of its assignment to a specific vibrational mode exists in the literature.

It is pertinent to study C–S, –C–O–C– and $-SO_3^-$ as group modes rather than single functional modes. A detailed investigation on changes in spectra with hydration and subsequent dehydration in the 800–1300 cm^{-1} would also provide helpful insights to accurately assign each of these peaks observed to specific vibrational modes.

3.2 Sulfonic acid group modes for dry Nafion

The vibrational spectrum of dry protonated form of Nafion was compared with the Na^+ form of dry Nafion by Negro *et al.*[44] The peak at 1410 cm^{-1} was absent in dry Nafion-Na^+ but was present in dry Nafion-H^+. This peak was therefore assigned to the antisymmetric stretching mode of $-SO_3H$ in the undissociated

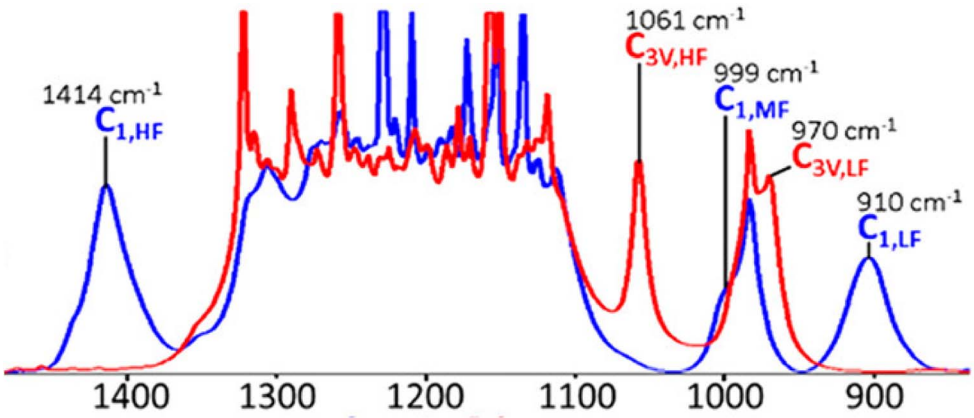

Fig. 8 DFT calculated spectra for fully dehydrated (blue) and fully hydrated membrane (red).[39] Reproduced with permission from ACS Publications.

form of Nafion.[44] This assignment was further supported by the disappearance of the sulfonic acid symmetric stretching mode at 1060 cm^{-1} on dehydration and simultaneous appearance of a peak at 1410 cm^{-1} [18,51,53] as shown in Fig. 8. C_1 stands for single functional modes while C_{3v} indicates coupled vibrational modes. DFT calculations also corroborated the assignment of 1414 cm^{-1} to the undissociated sulfonic acid.[34] The growth of the 1440 cm^{-1} band in treated membranes was accompanied by decreases in the intensities of water stretching and bending bands which are associated with the water molecules, which further supports this mode to be associated with dehydration of Nafion, anhydride formation.[45]

Contrary to the above studies, Los Alamos National Lab (LANL) did extensive investigation on the source of 1400 cm^{-1} mode observed in the FTIR of Nafion. Researchers at LANL could not see peaks at 1400 cm^{-1} irrespective of the membrane aging protocol followed.[46] Interestingly enough, LANL was able to reproduce this peak when they used Nylon as their material in their conditioning chamber. However, when using a 100% Teflon in the conditioning chamber, the peak was not present.[46]

Coms *et al.*,[47] in agreement with LANL, did not agree with the assignment of the 1440 cm^{-1} peak to undissociated $-SO_3H$ acid stretching mode and argued that if it was indeed anhydride, a peak near 750 cm^{-1} should have been observed. They found a blue shift in the 1440 cm^{-1} mode when Nafion was deuterated or exchanged with ammonium ions containing N14 and N15 isotopes. They argued that the 1440 cm^{-1} mode is a bending mode of water significantly red shifted due to a complex change in the structure of water channels on dehydration. LANL also ascribed this peak to the impurities in the system.[46]

Another peak at 2720 cm^{-1} is observed in Nafion. Since this peak shows a monotonic decrease with increasing hydration, it was ascribed to undissociated $-SO_3H$ by some groups.[42,48] Other groups assign at 2720 cm^{-1} mode to the Evans window (a local minimum resulting from various resonances) from overtones of bending modes and Fermi resonances.[18] Ferrari *et al.*[41] did not observe peaks at 1410 cm^{-1} mode, which is typical of $-SO_3H$, alongside 2720 cm^{-1} peak and therefore disfavored assignment of the 2720 cm^{-1} peak to the $-SO_3H$ mode.

The above studies indicate that the mode at 1400 cm^{-1} is likely not associated to anhydride formation as speculated. This peak also does not appear when Nafion is exchanged with sodium ions, but appears when exchanged with ammonium ions or deuterated water molecules. This implies that this mode could be related to the water molecules associating with the sulfonic acid groups. However, the limited number of studies performed on this subject makes it difficult to draw conclusions. Nevertheless, it seems like this mode is more complex than anhydride formation on Nafion drying speculated in the literature and needs to be further studied.

3.3 Changes in sidechain vibrational modes as a function of hydration

Proton transport in Nafion is widely accepted to occur *via* two mechanisms, vehicular and proton hopping. The proton hopping mechanism is prevalent under medium and lower levels of hydration when the protons are able to hop from one sulfonic site to the other. On the other hand, the vehicular or Grotthuss mechanism prevails under high levels of hydration and involves the transfer of protons by successive breaking and forming of covalent bonds across a chain of water molecules much like the transport of protons in bulk water.[9] The water transport mechanism in Nafion can be well interpreted by following the changes in the stretching modes of sulfonic acids and ether groups in the side chain as a function of hydration. The vibrational modes of the backbone are found to be unchanged with hydration. $-CF_2$ bending modes at 511 cm^{-1} and 626 cm^{-1} were found to be unaffected by hydration as also the mode at 983 cm^{-1}.[2,29]

Nafion FTIR spectra show two distinct peaks at 1740 cm^{-1} and 1630 cm^{-1}, which exhibit different behaviors during hydration/dehydration. 1650 cm^{-1} mode was assigned to water hydrogen bonding with other water molecules and sulfonic acid sites.[29] The 1720 cm^{-1} mode was assigned to water bound to protons.[35]

The mode at 1650 cm^{-1} is assigned to the highly confined hydronium ion for $3 \leq \lambda \leq 6$ which was found to shift to 1635 cm^{-1}, representing bulk water, as λ was further increased beyond 6. It was observed that sulfonic acid groups are completely dissociated for $1 \leq \lambda \leq 2$, which corresponds to 19% RH[49] in agreement with Ferrari *et al.*[41] who found complete dissociation of sulfonic acid groups for λ between 1.5 to 2. Leuchs and Zundel[50] also found that at sulfonic acid sites are completely dissociated $\lambda = 1.6$.

The mode at 1650 cm^{-1} disappears slowly on dehydration as shown in Fig. 9. When the membrane is completely dehydrated at 100 °C, no peaks are observed in the 1600 cm^{-1} region.[47] Peaks around 1600 cm^{-1} are the first to disappear on dehydration which is associated with the solvation sphere of water.[18] This implies that as the membrane is dehydrated, the non-hydrogen bonded free water reduces while the water tightly bonded to sulfonic acid remains even at low λ.

At 20% RH, surface diffusion of water is dominant. Water is tightly bound to $-SO_3^-$ up to 54% RH and the proton hopping is the dominant proton transport mode while Grotthuss diffusion is not present.[49] This was rationalized by the consistent presence of the 1720 cm^{-1} peak. Beyond 54% RH, water transitions to the bulk phase and can no longer exist as H_3O^+ and Grotthuss diffusion commences evident by the rise in intensity of the bulk water mode at 1635 cm^{-1} [49] as shown in Fig. 9.

In a completely dehydrated membrane, a peak is observed at 1440 cm^{-1}.[51] Lage *et al.*[30] observed peak broadening at 1060 cm^{-1} on drying which is attributed to internal dipole relaxation of –S–O as water is slowly removed. The mode at 1060 cm^{-1} vanishes in a completely dehydrated membrane with the simultaneous growth of the 1440 cm^{-1} mode.[18] The intensity of the asymmetric S–O stretching mode at 1210 cm^{-1} was found to increase with dehydration along with the simultaneous decrease in the symmetric –S–O stretching mode intensity at 1060 cm^{-1}, blue shifted to higher wavenumbers as hydration decreased.[52] Nuclear Magnetic Resonance (NMR) confirmed a strong correlation between membrane water content and $-SO_3^-$ symmetric stretching mode shifting.[30] The

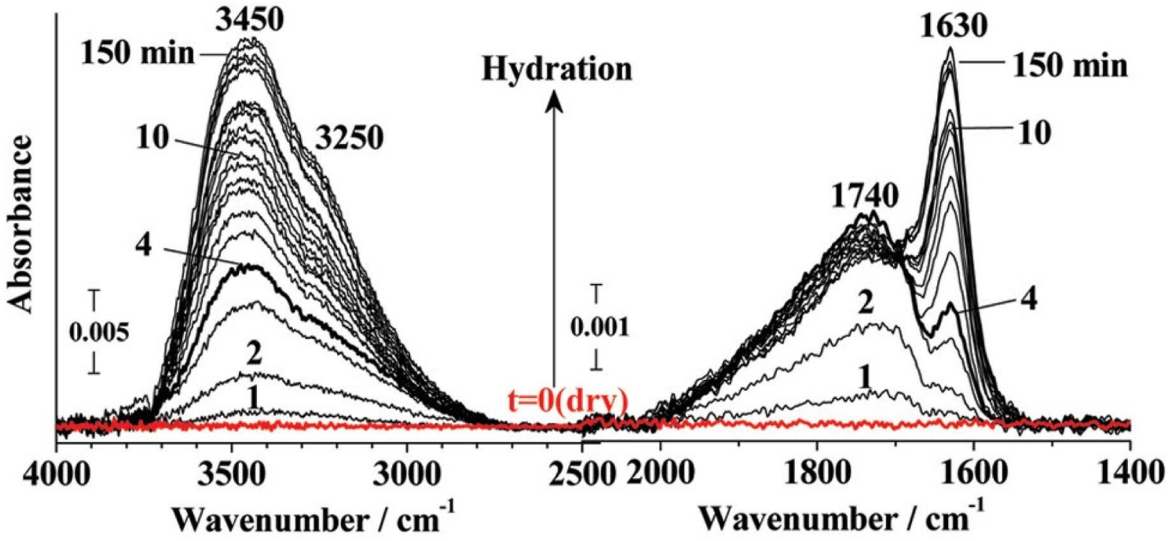

Fig. 9 Change in 1630 cm^{-1} and 1740 cm^{-1} peak with changing hydration.[35] Reproduced with permission from ACS Publications.

red shift in symmetric stretching mode of –S–O from 1063 cm^{-1} to 1057 cm^{-1} was found to be directly proportional to the jump in intensity at 1740 cm^{-1}. This explains that sulfonic acid groups are dissociated as hydration is increased.[35] It was found that ion pairs exist even at low water content ($\lambda = 1$ to 2),[49] however, the equilibrium starts shifting towards dissociation of the sulfonic acid group as the water content is increased.[30]

Conductivity was found to be directly proportional to the peak area at 1630 cm^{-1} ascribed to water strongly hydrogen bonded with other water molecules. Upon dehydration, the 1630 cm^{-1} mode disappears quickly while the 1740 cm^{-1} mode dies slowly, further supporting that proton conductivity results from dissociation of $-SO_3H$.[35]

In summary, the above studies reveal how FTIR has been used as a tool to validate the proton transport mechanisms and understand the influence of hydration on the proton transport pathways. Carefully monitoring the modes that change as a function of humidity has helped to rationalize the peak assignments and macroscale properties in Nafion. This is also why accurate assignment of vibrational modes to the various groups in Nafion is so critical to fully uncover the detailed structural characteristics of Nafion.

3.4 Influence of aging on vibrational spectra

Nafion properties are influenced by annealing and FTIR has been used to understand these changes. The influence of annealing on membrane water sorption as well as transport properties can be studied by monitoring changes in the vibrational modes of the side chain of Nafion.

Fig. 10 shows the changes in the various vibrational modes of Nafion when the membrane, pretreated with peroxide, is held in a climatic chamber at 80 °C and 80% RH over time. As evident from Fig. 10, aging reduces the intensity of the 1630 cm^{-1} peak which corresponds to bulk water. Simultaneously the peak intensity at 1410 cm^{-1} rises, showing that dehydration progresses with aging.[51,53] Shi *et al.*[54] found that the peak intensity at 1440 cm^{-1} increased more on aging in 75% RH compared to 100% RH showing more dehydration in lower RH conditions. Coms *et al.*[47] on the other hand, did not observe any degradation (change in 1440 cm^{-1} mode intensity) in air or N_2 for 100 h. They however performed degradation experiments by sandwiching the membrane between Teflon sheets before conditioning it in an oven as against Collette *et al.*[55] who performed the experiments with just the bare membrane. This aligns with the observations at LANL where no anhydride formation peak was evident when the membrane was aged by sandwiching between Teflon sheets. This further attests to the fact that the peak at 1440 cm^{-1} likely comes from contamination of sulfonic acid group.

After aging, partial regeneration of Nafion was found possible in liquid water but Nafion was found to be completely rejuvenated in acidic vapors confirmed by the reappearance of $-SO_3^-$ symmetric stretching mode at 1060 cm^{-1}.[51] Complete recovery of mechanical properties was observed after regeneration in 0.1 M acidic solution. With aging, the intensity of the 1710 cm^{-1} and 1630 cm^{-1} mode decreased while the intensity of the peak at 1440 cm^{-1} increased indicating decrease in water content upon aging as shown in Fig. 10.[51] This observation aligns with the findings of Kunimatsu *et al.*[35] who confirmed dehydration of the sample on aging.

Aging decreased the proton conductivity for various membranes owing to dehydration and subsequent loss in proton conductive sites ultimately leading to decreased water content. Changes in dissociated and undissociated sulfonic acid stretching mode at 1060 cm^{-1}, 1440 cm^{-1} respectively, and the peaks assigned to water stretching modes at 1630 cm^{-1} and 1700 cm^{-1} have been used to explain the changes in the water uptake and proton transport of Nafion when subjected to aging. The next section reviews studies of Nafion exchanged with cations to explore the effect of differing environment on Nafion vibrational modes and gain a deeper understanding of Nafion structure and transport properties.

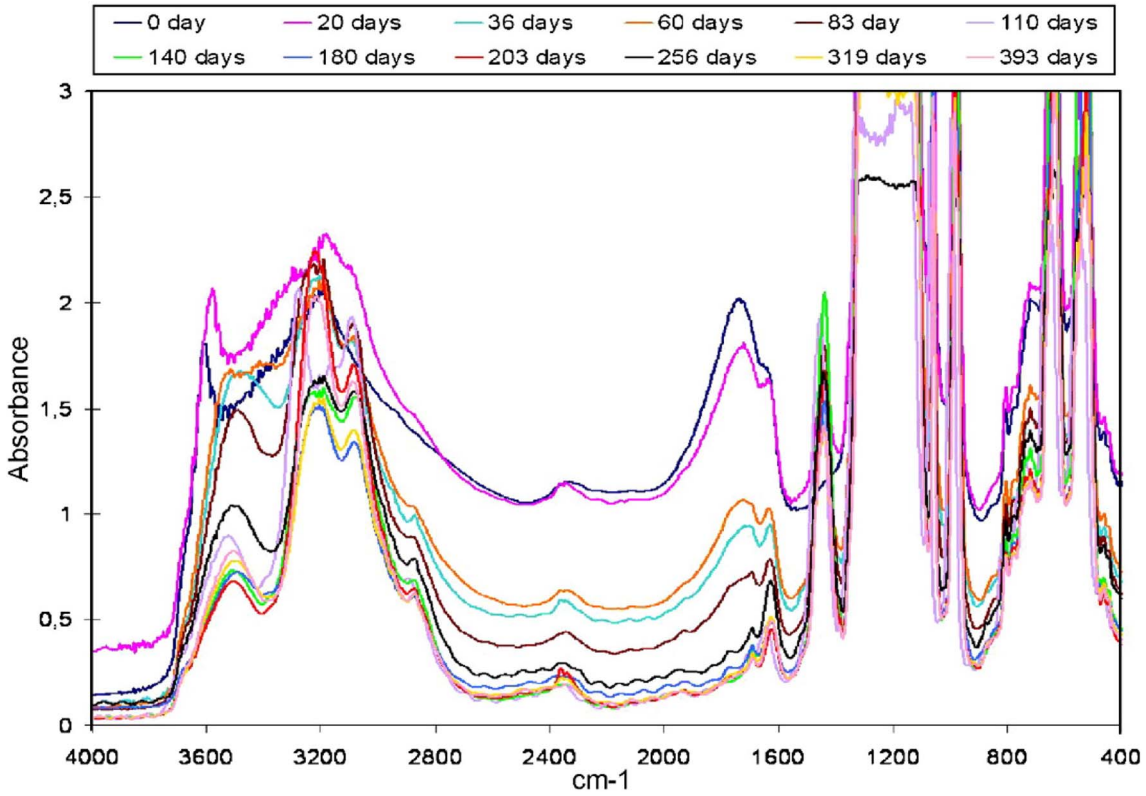

Fig. 10 Changes in Nafion IR spectrum as a function of aging time.[51] Reproduced with permission from Elsevier.

3.5 Effect of cations on membrane properties

Cations such as alkali metal ions, alkaline metal ions, and transition metal ions have differing hydration shell diameters and charge densities. Therefore, the ionic clusters formed when Nafion is exchanged with these ions are also markedly different. This is due to the differing water contents in the resulting membranes and cross-linking of the sulfonic acid groups by these high charge-density ions. Studying the FTIR spectra of Nafion exchanged with these cations can shed light on the formation of the ionic clusters and their structures. It is of particular interest to monitor the vibrational modes influenced by hydration on exchanging with these cations.

Sulfonic acid symmetric stretching is found to be strongly influenced by the counterion as shown in Fig. 11. The interactions between cations and the sulfonate groups in the fully hydrated Nafion membranes follow the order Li > Na > K > Rb > Cs for the alkali metal cations, and Ca > Sr > Ba > Mg for the alkaline earth metal cations.[56] The $-SO_3^-$ symmetric stretching mode at 1060 cm^{-1} was found to shift to higher wavenumbers as the alkaline metal ion radius increased due to reduced hydrogen bonding.[30] Li showed the strongest shift for the $-SO_3^-$ symmetric stretching mode, 1073 cm^{-1} for the dry sample and 1058 cm^{-1} for the wet sample[10] due to strong polarization of the –S–O group. Peak shifting of the $-SO_3^-$ mode also starts at lower mole fractions of cations for smaller cations compared to heavier cations.[10] Little or no shift for $-SO_3^-$ stretching vibrational mode was observed for large sized cations due to weak polarization.[10] For the 3M PFIA, symmetric stretching of the sulfonic acid group followed the order H^+ > Na > NH_4 > TEA showing the polarizing nature of these cations on the S–O group.[57] For organic cations, the trend was reversed with symmetric stretching mode of the S–O group moving to higher wavenumbers with increasing hydration. This suggests a complex structural behavior of Nafion in the presence of

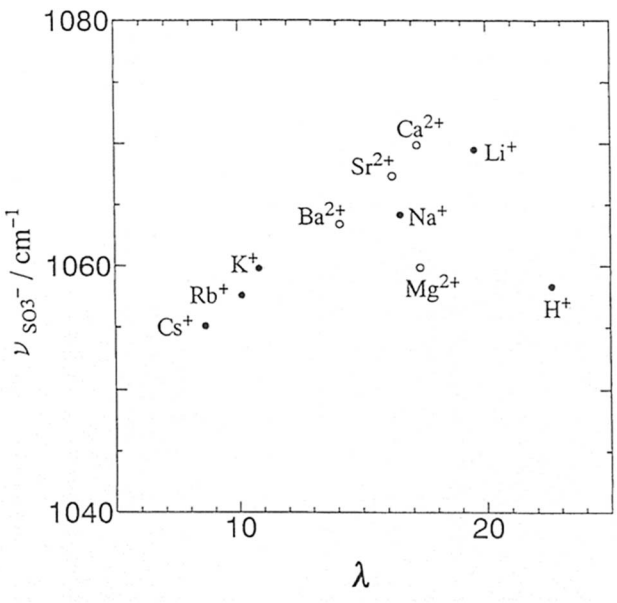

Fig. 11 Sulfonic acid symmetric stretching as a function of counterion.[56] Reproduced with permission from Marketplace™.

organic *vs.* inorganic cations and could result from the varying polarizability of the cation to $-SO_3^-$ or its preferential localization in hydrophobic regions of the membrane.[10]

Water permeability was found to be lower for membranes exchanged with metal ions because of their tendency to complex with $-SO_3H$ groups causing cross-linking of channels.[58] However, the effective water content of the membrane is a function of the cation type with higher charge density cations holding more water. For Li^+ and La^{3+} forms of Nafion, the bending mode for water at 1600 cm^{-1} in Nafion could be resolved into two distinct components as shown in Fig. 12. These split peaks were not observed for other cations.[59] These split bands indicate two distinct water environments for Nafion exchanged with these cations showing strong polarization effect resulting in a low frequency mode around 1616 cm^{-1} and a high frequency mode around 1629 cm^{-1}.[59]

The bending vibrational mode of water around 1650 cm^{-1} blue shifted with the decrease in cation radius due to increased H bonding.[30] The frequencies of the water stretching peak around 3690 cm^{-1} and 3500 cm^{-1} decrease with a decrease in cation radius. This was attributed to polymer contraction causing increased interaction with the –C–F backbone, and stronger interaction of the cation with water by hydrogen bonding, respectively.[30]

For the –O–H stretching region of Nafion, two vibrational peaks (A and B) were observed for cation exchanged membranes as shown in Fig. 13.[59,60]

Two distinct kinds of proton environments are possible in Nafion OH···F and OH···O, resulting in three different kinds of water environments, assigned as AA, BB, and AB. Peak A was ascribed to protons associated with the fluorocarbon backbone while peak B was ascribed to protons involved in hydrogen bonding. Therefore, AA refers to –O–H involved in hydrogen bonding with water molecules in the fluorocarbon phase A···OH···A, AB refers to –O–H involved in hydrogen bonding with water at the interface of the fluorocarbon and the bulk water and BB refers to –O–H hydrogen bonded to water in the bulk phase B···OH···B on both sides.[56] BB and AA peak formation was found to be correlated to the basic strength of the Lewis acid. AB is the predominant mode when the acid strength of the cation matches the acid strength of the sulfonate ion (=0.27), otherwise BB is found to predominate.[59]

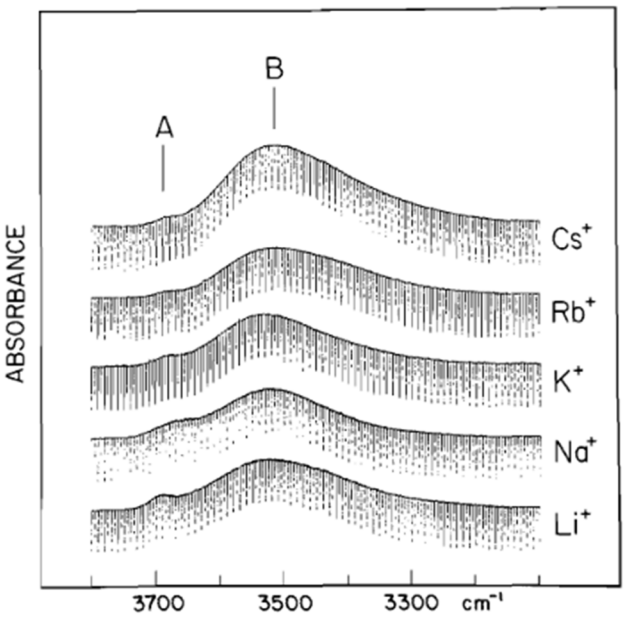

Fig. 13 Vibrational peaks for the –O–H stretching region of Nafion.[59] Reproduced with permission from Copyright clearance.

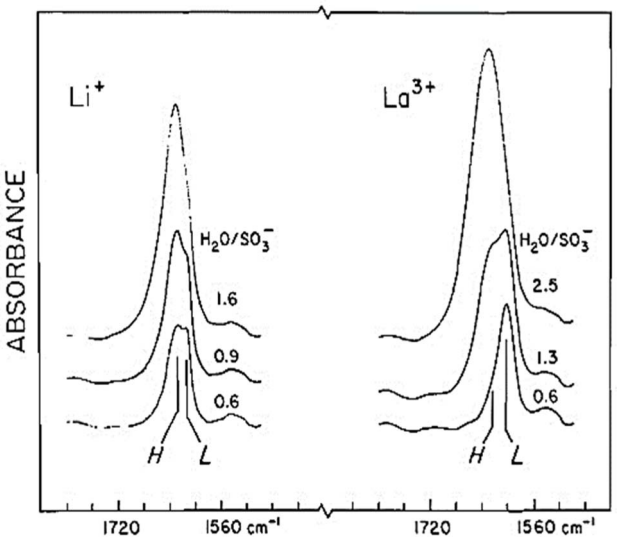

Fig. 12 Nafion spectrum for Li^+ and La^{3+} forms of Nafion.[59] Reproduced with permission from Copyright clearance.

The above studies show that the type of counterion (*viz.* its radius and charge density) significantly influences the water environment of Nafion. The interaction of the sidechain with the backbone is also affected by the type of counterion present in Nafion. It is also curious to note that no simple rule can explain the behavior of Nafion for all cation types, which again highlights the complex behavior of Nafion. For example, Mg^{2+} does not follow the expected trend of peak shifting for the $-SO_3^-$ symmetric stretching mode for which no explanation exists.[56] However, it is clear from the previous section that Nafion structural investigation becomes easier by exchanging Nafion with cations. For example, peak shifting of 1060 cm^{-1} with different cations confirm this mode is associated to $-SO_3^-$ stretching mode with contributions from –C–O–C– stretching possible. Further, the bending mode of water around 1600 cm^{-1} ascribed to bulk water in previous section, showed blue shifting with cation radius. This attests to the fact this mode likely represents bulk water phase in agreement with previous studies.

4 Vibrational modes of the Nafion backbone

Vibrational modes for the Nafion backbone corresponding to –CF–CF– were assigned by comparing Nafion's FTIR spectra with

that of PTFE as shown in Fig. 4. Vibrational modes for PTFE were observed at 505 cm^{-1}, 557 cm^{-1}, 628 cm^{-1}, 641 cm^{-1}, 1152 cm^{-1}, and 1206 cm^{-1}.[29] Therefore, the peaks observed in Nafion at these wavenumbers were assigned to –CF–CF– stretching modes in Nafion. The peak observed at 1120 cm^{-1} was assigned to –C–C symmetric stretching.[40] The peaks at 1108 cm^{-1} was ascribed to –C–F stretching[40] while the peaks at 1156 cm^{-1} and 1229 cm^{-1} were assigned to the symmetric and asymmetric C–F stretching, respectively.[29] The assignment of vibrational modes to Nafion backbone is straightforward and not complicated by overlapping peaks and interference from other vibrational modes as discussed in the past section.

5 OH vibrational region of Nafion

Proton transport and preventing gases on the anode and cathode sides from mixing with each other are the two critical functions of the electrolyte in fuel cells and electrolyzers. Nafion exists as a phase-segregated structure comprising the main hydrophobic backbone and ionic sidechains. This has implications for proton transport which varies with the degree of hydration. IR pump probe spectroscopy indicated that the energy levels of the modes within Nafion are correlated with their vibrational lifetimes. Two vibrational lifetimes were observed for $\lambda = 3$ at 3.2 ps and 8.6 ps strongly suggesting that Nafion has two different kind of water environments. The vibrational lifetimes were found to change with hydration suggesting that there is restructuring of the hydrophilic domain with hydration.[61] Therefore, understanding the changes in OH vibrational modes with hydration is instrumental in understanding the changes in the membrane's proton transport channels and proton transport mechanisms with varying λ.[62]

5.1 Assignment of frequencies

As the water content in the membrane changes, so do the interactions of water with the various functional groups in Nafion. This also modifies the –OH stretching modes observed in Nafion. Therefore, changes in the water bending and stretching modes can serve as effective probes for the effect of hydration on Nafion's transport properties. The vibrational spectra for –OH in Nafion is, however, not straightforward. It is complicated by the overlapping from overtones of lower frequency modes and Fermi resonances resulting from two vibrational modes appearing at the same frequency.[18] Studying the deuterium-substituted OD stretching is useful for deconvoluting the overlapped peaks observed in the spectra. The mass effect causes the hydroxyl stretching of the deuterium-substituted group, OD, to be red-shifted to around 2500 cm^{-1} relative to the OH stretch which helps in data analysis.

The infrared spectrum of HOD in liquid water was compared to Nafion. Two peaks were observed at 3660 cm^{-1} (Peak A) and 3520 cm^{-1} (Peak B) as shown in Fig. 13 suggesting two different kinds of water surroundings in Nafion.[59,63,64] This was also implied by the observation of two peaks at 1740 cm^{-1} and 1630 cm^{-1} in the sidechain vibrational region of Nafion.[35] HOD was impregnated in Nafion to verify the assignment of frequencies in the 3000 cm^{-1} to 4000 cm^{-1} range. Since HOD has distinct asymmetric and symmetric modes dominated by OD and OH stretching respectively, resolution of the peaks is easier. Using this strategy, it was found that the 3668 cm^{-1} mode is the symmetric stretching mode of HOD with the OH bond directed towards the hydrophobic phase.[65] 3520 cm^{-1} mode was assigned to water hydrogen bonding with other water molecules blue shifted from 3400 cm^{-1} compared to bulk water due to weaker hydrogen bonding interactions.[66]

Ferrari *et al.*[41] observed two peaks at 3005 cm^{-1} and 3280 cm^{-1} for dehydrated Nafion. At 5% RH, a peak was observed at 3470 cm^{-1} which was assigned to less strongly bonded water molecules. As the RH was increased to 40%, another peak at 3515 cm^{-1} started appearing.[41] Peak at 3700 cm^{-1} was assigned to the free OH group.[64] This mode was also observed by Falk *et al.*[60] and was ascribed to AA interactions referring to water primarily in the fluorocarbon phase and shown in Fig. 13. This peak was later assigned to the OH stretching mode for interfacial water by Hofmann *et al.*[67]

Several other peaks were observed in this region by various groups. Laporta *et al.*[68] assigned the peak at 3370 cm^{-1} to the OH stretching of residual water in the membrane after dehydration. Peaks at 3414 cm^{-1} and 3202 cm^{-1} were assigned to the water-free H_3O^+ mode, due to their presence with the peak at 1700 cm^{-1} ascribed to hydronium ions strongly hydrogen bonded to sulfonate.[29] This aligns with the observations of Ferrari *et al.*[41] who observed peaks at 3280 cm^{-1} and 3470 cm^{-1} for a dehydrated Nafion. A peak at 3400 cm^{-1} was observed for triflic acid associated with two water molecules.[69] This further attests that the peaks around 3400 cm^{-1} in Nafion are indicative of low water content tightly bound to sulfonic acid sites. Basnayake *et al.*[64] observed that on dehydration, the peak at 3690 cm^{-1} ascribed to interfacial OH stretching mode diminishes and a sharp peak at 2670 cm^{-1} appears. This agrees with the results from Ren *et al.*[69] who observed a peak at 2800 cm^{-1} for triflic acid with $\lambda = 1$, nearly dehydrated state. H_3O^+ strongly H-bonded to sulfonate was assigned to 2980 cm^{-1} mode in the previous section.[29] On complete dehydration, the peak at 2750 cm^{-1} vanished and new modes at 3012 cm^{-1} and 1410 cm^{-1} appeared.[64] In another study by Ren *et al.*,[69] triflic acid was used for understanding the different water states of Nafion. The peak at 3000 cm^{-1} present in dehydrated Nafion is indicative of regions with densely packed sulfonic acid groups[18] in alignment with the findings of other groups.[67]

Modes in the 3500 cm^{-1} to 3700 cm^{-1} region were also observed for thin films on hydration.[70] A rise in the peak intensities of A and B was observed as RH was increased, and when RH reached 100%, a broad peak at 3500 cm^{-1} appeared which was assigned to bulk water. Intensity changes of the OH stretching modes for Nafion were recorded as a function of humidity.[71,72] Peaks at 3525 cm^{-1} and 3674 cm^{-1} were found to increase with humidity following similar trends which suggests that both these vibrational modes come from bulk water and water in both these modes rapidly equilibrate on hydration.[64]

A higher frequency peak observed at 3810 cm^{-1} was ascribed to water molecules weakly hydrogen bonded to SO_3^- by Basnayake *et al.*[64] This seems to be an imprecise assignment since

the H bonding interactions of OH with the sulfonic acid group might be stronger than the fluorocarbon chain and probably should have arisen at lower frequencies. Hofmann *et al.*[67] ascribed the two modes at 3459 cm^{-1} and 3287 cm^{-1} to the antisymmetric and symmetric stretching modes of bulk-like water in Nafion. Bulk water peaks have been observed above 3500 cm^{-1} in other studies.[29,35,64] This also contradicts the dehydration studies of Nafion discussed above.

The above literature review indicates that a general consensus in the community on the assignment of vibration modes above 3500 cm^{-1} are attributed to the highly hydrated form of Nafion, and modes below 3500 cm^{-1} are observed for lower levels of hydration where water is tightly bound to the sulfonic acid group. These vibrational modes closely follow the growth of modes in 1600 cm^{-1} and 1700 cm^{-1} region which in turn closely follow the growth of mode at 1060 cm^{-1}. This strong correlation of various vibrational modes with each other and with hydration has helped understand the water transport in Nafion over the decades and uncover the properties of the water transport channels. For example, the simultaneous rise of peak intensity at 1057 cm^{-1}, 1650 cm^{-1} and at 3500 cm^{-1} for a given λ helped understand the change in proton transport mechanism from proton hopping to Grotthuss and the underlying reasons for the behavior.

The next section will discuss studies that used the knowledge from IR spectra to understand the mode of ionic and water transport channels in Nafion, and the structure of water transport channels.

6 Water transport behavior in Nafion

By closely following the appearance and disappearance of vibrational modes assigned to OH stretching and side chains, inferences can be made about proton transport mechanisms at different degrees of hydration. Water content in Nafion for a given λ and humidity can also be estimated precisely by measuring the relative peak areas for the vibrational modes of interest. Synthesizing this knowledge with the ionic cluster size and shape calculations from other techniques can help validate the assumptions made about the water transport channels. Some interesting studies in this area are highlighted below.

From the relative absorbance of water vibrational modes at 3500 cm^{-1} and 3600 cm^{-1}, the ratio of bulk water to water at the interface of fluorocarbon phase was estimated to be about 13 : 4.[60] As the hydration increased, the –OH stretching peak intensity for AA band decreased sharply causing Falk *et al.*[60] to hypothesize that the ionic clusters must have a high surface area to volume ratio. Hsu *et al.*[73] estimated the ionic clusters to be spherical with a diameter of 40 Å with an intercluster distance of 50 Å from XRD studies. However, the high surface area to volume ratio found by Falk *et al.*[60] implies that the clusters are either very small or non-spherical in shape.

For $\lambda = 1$, Ludvigsson *et al.*[74] found that SO_3^- is tightly bonded to the H_3O^+ ion confirmed by the broad peak at 2800 cm^{-1} which is typical of H_3O^+ bound tightly to sulfonic acid group. Peaks at 1410 cm^{-1} and 927 cm^{-1} assigned to S=O stretching were absent further confirming that the sulfonic acid is dissociated. As λ was increased to 2, a broad peak at 3450 cm^{-1} appears, typical of associated water. As the water content was increased beyond $\lambda = 3$, the water bending mode starts appearing around 1630 cm^{-1} [68,74] indicative of bulk like water. Continuous rise in absorbance was observed for the water bending mode with increase in λ.[35,68] FTIR data therefore suggests that Nafion shows continuous channel formation around $\lambda = 5$ to 6.[68] Continuous channels, however, cannot form for spherical or cylindrical channels until $\lambda = 8$.[68] It was therefore found that Nafion ionic channels exist as cylindrical and spherical structures only in extreme cases and the channels are usually distorted in shape. Channels formation in Nafion was also supported by other studies.[68,75,76]

Polarization selective pulse probe combined with IR vibrational echo spectroscopy was used to investigate the water transport mechanism in Nafion.[62] The relative decay of water in 2D IR was found to be 2.4 ps for the core and 5.9 ps for the interface, which is similar to the aerosol-OT reverse micelle (RM). The core lifetime was longer as compared to 1.8 ps for bulk water which implied a weaker hydrogen bonding in the core. This was also suggested by the blue shift of OH stretching from 3400 cm^{-1} for bulk water to 3520 cm^{-1} for water in Nafion.[66] The calculated RMS diameter of water clusters was found greater than 60 Å for Nafion which is much larger than the other studies.[73] The orientational time was also found to be longer than predicted by other studies. Roget *et al.*[62] interpreted this as water channels existing as parallel cylindrical structures of 24 Å on short scale instead of spherical clusters.

Ling *et al.*[77] calculated the concentration of OH in various membranes from the absorbance value in FTIR, and fitted Fick's second law to the time-dependent data. They found that for all the different membranes tested, total OH diffusivity was found to be proportional to the interfacial water diffusivity irrespective of the ratio of the bulk/non-bulk water obtained from FTIR. They also found that non-bulk water is dominant in smaller channels while bulk water is dominant in larger channels due to higher hydrogen bonding. Membranes with higher concentrations of smaller ionic clusters are expected to show higher proton conductivity. Roget *et al.*[62] found that core water in Nafion is the main proton conduction mechanism while Tsuneda *et al.*[37] found excellent agreement between theory and experiment when they assumed a relay mechanism/vehicular transport for water transport. It therefore appears that protonated water clusters are the main source of proton transport.[62,77] Hallinan *et al.*[31] found that at low RH (0–22%), water exhibits non-Fickian behavior in Nafion. As water is associated to SO_3^-, a time lag occurs between water absorption and its conversion to protonated water, resulting in non-fickian behavior. The time lag increased with decreasing λ, which is expected.

Nafion was found to exhibit different surface and bulk structure.[78] When ATR was compared to transmission spectra of Nafion after thermal treatment, –SO_3H and –C–O–C– peak areas increased with respect to –CF_2 which implied that sidechains move to the surface on annealing. It was hypothesized due to cluster aggregation and shrinkage.[78] It was found that thermal treatment changes the membrane from micellar to inverted

micellar form based on the blue shift of the symmetric stretching vibration of $-SO_3^-$ to 1070 cm^{-1}.[78]

Hara *et al.*[33] found that the areal ratio of –S–O vibrations (around 1058 cm^{-1}) to C–F (around 731 cm^{-1}) was higher in an operating cell than in the 30% RH standing test, which proved large retention of water in the catalyst layers, and also provided evidence for back diffusion of water from cathode to anode. On increasing temperature at 30% RH, the intensity ratio of S–O/C–F increased showing increasing water diffusion.

7 Conclusions

This paper presents a comprehensive review on the use of infrared spectroscopy to understand the structure and properties of Nafion and understand its degradation by following relevant vibrational modes . This review provides a brief overview of the potential of FTIR to provide deep insights into material level and sometimes system level effects when appropriate understanding of the materials vibrational spectrum is present. FTIR spectroscopy has been used across a wide range of studies to understand the mechanism of water transport in Nafion, draw inferences about the structure of Nafion's water transport channels, evaluate the diffusion and sorption kinetics in Nafion, and understand the movement of water in an operating fuel cell. Verifying FTIR observations with data from other techniques has helped to validate assumptions and gain greater insights into transport mechanisms in Nafion.

There are, however, research gaps in terms of some of the assignments in Nafion FTIR spectrum. Despite extensive modeling and comparison studies with model compounds, the literature reveals a lack of consensus on the assignment of 983 cm^{-1} and 800 cm^{-1} mode. 983 cm^{-1} is a humidity independent mode and has been assigned to $-CF_2$ stretching mode or –C–O–C stretching mode in sidechain by differing groups. The C–S mode is spread between 800–1200 cm^{-1} and strongly coupled to the sulfonic acid and ether modes. It has been associated to 800 cm^{-1}, 980 cm^{-1} and 1180 cm^{-1} with no accepted assignment to date. Effect of organic cations on Nafion side chain vibrational modes need to be investigated further. Much of the knowledge of sulfonic acid symmetric stretching mode shifting with alkali and alkaline metal ions exists but similar understanding is non-existent for organic cations. Organic cations are used to change processability of Nafion for varied applications and understanding their impact on Nafion properties and structure would advance those areas.

Disagreements still exists about the peak assignment of 1440 cm^{-1} mode observed in FTIR. It is still widely believed to be due to anhydride formation. However, this mode was found to be absent when Nafion is investigated under conditions where impurities are eliminated. This raises questions about this assignment and needs further experimental and computational studies to identify the source of this vibrational mode.

General agreement exists in the assignment of –OH stretching modes in Nafion. The peaks above 3500 cm^{-1} are attributed to the highly hydrated form of Nafion, and peaks below 3500 cm^{-1} are observed for lower levels of hydration where water is tightly bound to the sulfonic acid group. However, there are modes that are observed by some groups but not by others like the 3000 cm^{-1} and 2800 cm^{-1}mode. This stems from inaccurate measurement of hydration for the membranes which could change observations between groups. More work is needed on the interfacial to bulk water dynamics in Nafion with hydration level which is fundamental to Nafion proton transport properties. Future work should also focus on modeling studies with experimental validation that would allow comparison between studies from different groups. Pretreatment and measurement conditions of Nafion should be reported clearly by researchers to enable accurate use of published information.

With the advancements in FTIR technology, one can anticipate using this technique for a host of other applications. The potential of infrared spectroscopy in applications like hydrogen fuel cells continues to remain strong considering the ease of use and availability that the technique offers as against other more demanding techniques like X-ray scattering or neutron scattering.

Conflicts of interest

There are no conflicts to declare.

Acknowledgements

Los Alamos National Laboratory acknowledges the U.S. Department of Energy, Office of Energy Efficiency and Renewable Energy, and Hydrogen and Fuel Cell Technologies Office who supported this research through the Million Mile Fuel Cell Truck Consortium and technology managers G. Kleen and D. Papageorgopoulos. The University of Delaware acknowledges The Chemours Company for providing an Applied Research Grant to support this work.

References

1 W. Grot, Use of Nafion Perfluorosulfonic Acid Products as Separators in Electrolytic Cells, *Chem.-Ing.-Tech.*, 1978, **50**(4), 299–301, DOI: 10.1002/cite.330500415.
2 C. Korzeniewski, E. Adams and D. Liu, Responses of hydrophobic and hydrophilic groups in Nafion differentiated by least squares modeling of infrared spectra recorded during thin film hydration, *Appl. Spectrosc.*, 2008, **62**(6), 634–639, DOI: 10.1366/000370208784658075.
3 A. V. Petrov and I. V. Murin, Electronic Structure of SO3H Functional Groups and Proton Mobility in Nafion and Aquivion Ionomer Membranes, *Russ. J. Gen. Chem.*, 2019, **89**(3), 553–555, DOI: 10.1134/S1070363219030320.
4 N. Yoshida, T. Ishisaki, A. Watakabe and M. Yoshitake, Characterization of Flemion (R) membranes for PEFC, *Electrochim. Acta*, 1998, **43**(24), 3749–3754, DOI: 10.1016/S0013-4686(98)00133-9.
5 L. J. Salazar-Gastelum, B. Y. Garcia-Limon, S. W. Lin, J. C. Calva-Yanez, A. Zizumbo-Lopez, T. Romero-Castanon, M. I. Salazar-Gastelum and S. Perez-Sicairos, Synthesis of Anion Exchange Membranes Containing PVDF/PES and

Either PEI or Fumion (R), *Membranes*, 2022, **12**(10), 959, DOI: 10.3390/membranes12100959.

6 D. Brandell, J. Karo, A. Liivat and J. O. Thomas, Molecular dynamics studies of the Nafion (R), Dow (R) and Aciplex (R) fuel-cell polymer membrane systems, *J. Mol. Model.*, 2007, **13**(10), 1039–1046, DOI: 10.1007/s00894-007-0230-7.

7 U. N. Shrivastava, H. Fritzsche and K. Karan, Interfacial and Bulk Water in Ultrathin Films of Nafion, 3M PFSA, and 3M PFIA Ionomers on a Polycrystalline Platinum Surface, *Macromolecules*, 2018, **51**(23), 9839–9849, DOI: 10.1021/acs.macromol.8b01240.

8 T. F. Fuller and J. Newman, Experimental-Determination of the Transport Number of Water in Nafion-117 Membrane, *J. Electrochem. Soc.*, 1992, **139**(5), 1332–1337, DOI: 10.1149/1.2069407.

9 A. Kusoglu and A. Z. Weber, New Insights into Perfluorinated Sulfonic-Acid Ionomers, *Chem. Rev.*, 2017, **117**(3), 987–1104, DOI: 10.1021/acs.chemrev.6b00159.

10 S. R. Lowry and K. A. Mauritz, An Investigation of Ionic Hydration Effects in Perfluorosulfonate Ionomers by Fourier-Transform Infrared-Spectroscopy, *J. Am. Chem. Soc.*, 1980, **102**(14), 4665–4667, DOI: 10.1021/ja00534a017.

11 J. A. Elliott, D. S. Wu, S. J. Paddison and R. B. Moore, A unified morphological description of Nafion membranes from SAXS and mesoscale simulations, *Soft Matter*, 2011, **7**(15), 6820–6827, DOI: 10.1039/c1sm00002k.

12 S. J. Berens, A. Yahya, J. C. Fang, A. Angelopoulos, J. D. Nickels and S. Vasenkov, Transition between Different Diffusion Regimes and Its Relationship with Structural Properties in Nafion by High Field Diffusion NMR in Combination with Small-Angle X-ray and Neutron Scattering, *J. Phys. Chem. B*, 2020, **124**(40), 8943–8950, DOI: 10.1021/acs.jpcb.0c07249.

13 S. C. DeCaluwe, P. A. Kienzle, P. Bhargava, A. M. Baker and J. A. Dura, Phase segregation of sulfonate groups in Nafion interface lamellae, quantified via neutron reflectometry fitting techniques for multi-layered structures, *Soft Matter*, 2014, **10**(31), 5763–5776, DOI: 10.1039/c4sm00850b.

14 V. S. Murthi, J. A. Dura, S. Satija and C. F. Majkrzak, Water Uptake and Interfacial Structural Changes of Thin Film Nafion (R) Membranes Measured by Neutron Reflectivity for PEM Fuel Cells, *Proton Exchange Membrane Fuel Cells 8, Pts 1 and 2*, 2008, **16**(2), 1471, DOI: 10.1149/1.2981988.

15 S. K. Young, S. F. Trevino and N. C. B. Tan, Small-angle neutron scattering investigation of structural changes in Nafion membranes induced by swelling with various solvents, *J. Polym. Sci., Polym. Phys.*, 2002, **40**(4), 387–400, DOI: 10.1002/polb.10092.

16 A. A. Bunaciu, H. Y. Aboul-Enein and V. D. Hoang, *Vibrational Spectroscopy Applications in Biomedical, Pharmaceutical and Food Sciences*, Elsevier, 2020.

17 *Spectroscopic methods for nanomaterials characterization*, ed. S. Thomas, R. Thomas, A. K. Zachariah and R. Kumar, Elsevier, 2017, vol. 2, pp. 1–424.

18 R. Buzzoni, S. Bordiga, G. Ricchiardi, G. Spoto and A. Zecchina, Interaction of H2o, Ch3oh, (Ch3)(2)O, Ch3cn, and Pyridine with the Superacid Perfluorosulfonic Membrane Nafion - an Ir and Raman-Study, *J. Phys. Chem.*, 1995, **99**(31), 11937–11951, DOI: 10.1021/j100031a023.

19 M. Danilczuk, L. Lin, S. Schlick, S. J. Hamrock and M. S. Schaberg, Understanding the fingerprint region in the infra-red spectra of perfluorinated ionomer membranes and corresponding model compounds: Experiments and theoretical calculations, *J. Power Sources*, 2011, **196**(20), 8216–8224, DOI: 10.1016/j.jpowsour.2011.05.067.

20 D. S. Warren and A. J. McQuillan, Infrared spectroscopic and DFT vibrational mode study of perfluoro(2-ethoxyethane) sulfonic acid (PES), a model Nafion side-chain molecule, *J. Phys. Chem. B*, 2008, **112**(34), 10535–10543, DOI: 10.1021/jp801838n.

21 K. A. Mauritz and R. B. Moore, State of understanding of Nafion, *Chem. Rev.*, 2004, **104**(10), 4535–4585, DOI: 10.1021/cr0207123.

22 O. N. Primachenko, E. A. Marinenko, A. S. Odinokov, S. V. Kononova, Y. V. Kulvelis and V. T. Lebedev, State of the art and prospects in the development of proton-conducting perfluorinated membranes with short side chains: A review, *Polym. Adv. Technol.*, 2021, **32**(4), 1386–1408, DOI: 10.1002/pat.5191.

23 M. A. Hickner and B. S. Pivovar, The chemical and structural nature of proton exchange membrane fuel cell properties, *Fuel Cells*, 2005, **5**(2), 213–229, DOI: 10.1002/fuce.200400064.

24 A. J. Duncan, D. J. Leo and T. E. Long, Beyond Nafion: Charged Macromolecules Tailored for Performance as Ionic Polymer Transducers, *Macromolecules*, 2008, **41**(21), 7765–7775, DOI: 10.1021/ma800956v.

25 S. Y. Choi, M. M. Ikhsan, K. S. Jin and D. Henkensmeier, Nanostructure-property relationship of two perfluorinated sulfonic acid (PFSA) membranes, *Int. J. Energy Res.*, 2022, **46**(8), 11265–11277, DOI: 10.1002/er.7926.

26 P. C. Okonkwo, I. Ben Belgacem, W. Emori and P. C. Uzoma, Nafion degradation mechanisms in proton exchange membrane fuel cell (PEMFC) system: A review, *Int. J. Hydrogen Energy*, 2021, **46**(55), 27956–27973, DOI: 10.1016/j.ijhydene.2021.06.032.

27 X. H. Yan, Z. L. Xu, S. Yuan, A. D. Han, Y. T. Shen, X. J. Cheng, Y. W. Liang, S. Y. Shen and J. L. Zhang, Structural and transport properties of ultrathin perfluorosulfonic acid ionomer film in proton exchange membrane fuel cell catalyst layer: A review, *J. Power Sources*, 2022, **536**, 231523, DOI: 10.1016/j.jpowsour.2022.231523.

28 M. Laporta, M. Pegoraro and L. Zanderighi, Perfluorosulfonated membrane (Nafion): FT-IR study of the state of water with increasing humidity, *Phys. Chem. Chem. Phys.*, 1999, **1**(19), 4619–4628, DOI: 10.1039/a904460d.

29 A. Gruger, A. Regis, T. Schmatko and P. Colomban, Nanostructure of Nafion (R) membranes at different states of hydration - An IR and Raman study, *Vib. Spectrosc.*, 2001, **26**(2), 215–225, DOI: 10.1016/S0924-2031(01)00116-3.

30 L. G. Lage, P. G. Delgado and Y. Kawano, Vibrational and thermal characterization of Nafion (R) membranes

substituted by alkaline earth cations, *Eur. Polym. J.*, 2004, **40**(7), 1309–1316, DOI: 10.1016/j.europolymj.2004.02.021.

31 D. T. Hallinan, M. G. De Angelis, M. G. Baschetti, G. C. Sarti and Y. A. Elabd, Non-Fickian Diffusion of Water in Nafion, *Macromolecules*, 2010, **43**(10), 4667–4678, DOI: 10.1021/ma100047z.

32 C. Heitnerwirguin, Infrared-Spectra of Perfluorinated Cation-Exchanged Membranes, *Polymer*, 1979, **20**(3), 371–374, DOI: 10.1016/0032-3861(79)90103-4.

33 M. Hara, J. Inukai, K. Miyatake, H. Uchida and M. Watanabe, Temperature dependence of the water distribution inside a Nafion membrane in an operating polymer electrolyte fuel cell. A micro-Raman study, *Electrochim. Acta*, 2011, **58**, 449–455, DOI: 10.1016/j.electacta.2011.09.067.

34 M. Lopez, B. Kipling and H. L. Yeager, Exchange-Rates and Water-Content of a Cation-Exchange Membrane in Aprotic-Solvents, *Anal. Chem.*, 1976, **48**(8), 1120–1122, DOI: 10.1021/ac50002a014.

35 K. Kunimatsu, B. Bae, K. Miyatake, H. Uchida and M. Watanabe, ATR-FTIR Study of Water in Nafion Membrane Combined with Proton Conductivity Measurements during Hydration/Dehydration Cycle, *J. Phys. Chem. B*, 2011, **115**(15), 4315–4321, DOI: 10.1021/jp112300c.

36 M. Webber, N. Dimakis, D. Kumari, M. Fuccillo and E. S. Smotkin, Mechanically Coupled Internal Coordinates of Ionomer Vibrational Modes, *Macromolecules*, 2010, **43**(13), 5500–5502, DOI: 10.1021/ma100915u.

37 T. Tsuneda, R. K. Singh, A. Iiyama and K. Miyatake, Theoretical Investigation of the H2O2-Induced Degradation Mechanism of Hydrated Nafion Membrane via Ether-Linkage Dissociation, *ACS Omega*, 2017, **2**(7), 4053–4064, DOI: 10.1021/acsomega.7b00594.

38 Y. Okamoto, An ab initio study of the side chain of Nafion, *Chem. Phys. Lett.*, 2004, **389**(1–3), 64–67, DOI: 10.1016/j.cplett.2004.03.060.

39 N. Loupe, K. Abu-Hakmeh, S. Gao, L. Gonzalez, M. Ingargiola, K. Mathiowetz, R. Cruse, J. Doan, A. Schide, I. Salas, N. Dimakis, S. S. Jang, W. A. Goddard III and E. S. Smotkin, Group Vibrational Mode Assignments as a Broadly Applicable Tool for Characterizing Ionomer Membrane Structure as a Function of Degree of Hydration, *Chem. Mater.*, 2020, **32**(5), 1828–1843.

40 A. J. Aquino and D. Tunega, Ab Initio Molecular Dynamics Simulations on the Hydrated Structures of Na+–Nafion Models, *J. Phys. Chem. C*, 2017, **121**(21), 11215–11225.

41 M. C. Ferrari, J. Catalano, M. G. Baschetti, M. G. De Angelis and G. C. Sarti, FTIR-ATR Study of Water Distribution in a Short-Side-Chain PFSI Membrane, *Macromolecules*, 2012, **45**(4), 1901–1912, DOI: 10.1021/ma202099p.

42 A. Narebska and J. Ostrowska, Infrared study of hydration and association of functional groups in a perfluorinated Nation membrane, Part I, *Colloid Polym. Sci.*, 1983, **261**, 93–98.

43 J. Etheve, P. Huguet, C. Innocent, J. L. Bribes and G. Pourcelly, Electrochemical and Raman spectroscopy study of a Nafion perfluorosulfonic membrane in organic solvent-water mixtures, *J. Phys. Chem. B*, 2001, **105**(19), 4151–4154, DOI: 10.1021/jp003642h.

44 E. Negro, M. Vittadello, K. Vezzu, S. J. Paddison and V. Noto, The influence of the cationic form and degree of hydration on the structure of Nafion (TM), *Solid State Ionics*, 2013, **252**, 84–92, DOI: 10.1016/j.ssi.2013.09.017.

45 S. M. Clapham, F. D. Coms, T. J. Fuller and L. Zou, Degradation of perfluorosulfonic acid membrane water permeance via formation of sulfonic acid anhydrides, *ECS Trans.*, 2013, **50**(2), 1011.

46 K. C. R. Rod Borup, *Anhydride Formation on Aged N211 and N212 Membranes*, 2012.

47 F. D. Coms, T. J. Fuller and C. P. Schaffer, A Mechanistic Study of Perfluorosulfonic Acid Membrane Water Permeance Degradation in Air, *J. Electrochem. Soc.*, 2018, **165**(6), F3104–F3110, DOI: 10.1149/2.0141806jes.

48 K. O. Reikichi Iwamoto, M. Sato and Y. Iseki, Water in perfluorinated sulfonic acid Nafion membranes, *J. Phys. Chem. B*, 2002, **106**(28), 6973–6979.

49 L. Grosmaire, S. Castagnoni, P. Huguet, P. Sistat, M. Boucher, P. Bouchard, P. Bebin and S. Deabate, Probing proton dissociation in ionic polymers by means of in situ ATR-FTIR spectroscopy, *Phys. Chem. Chem. Phys.*, 2008, **10**(11), 1577–1583, DOI: 10.1039/b714870d.

50 M. Leuchs and G. Zundel, Easily polarizable hydrogen bonds in aqueous solutions of acids. Perchloric acid and trifluoromethane sulphonic acid, *J. Chem. Soc., Faraday Trans. 2*, 1978, **74**, 2256–2267.

51 F. M. Collette, C. Lorentz, G. Gebel and F. Thominette, Hygrothermal aging of Nafion (R), *J. Membr. Sci.*, 2009, **330**(1–2), 21–29, DOI: 10.1016/j.memsci.2008.11.048.

52 R. K. Singh, K. Kunimatsu, K. Miyatake and T. Tsuneda, Experimental and Theoretical Infrared Spectroscopic Study on Hydrated Nafion Membrane, *Macromolecules*, 2016, **49**(17), 6621–6629, DOI: 10.1021/acs.macromol.6b00999.

53 J. L. Qiao, M. Saito, K. Hayamizu and T. Okada, Degradation of perfluorinated ionomer membranes for PEM fuel cells during processing with H2O2, *J. Electrochem. Soc.*, 2006, **153**(6), A967–A974, DOI: 10.1149/1.2186768.

54 S. Shi, T. J. Dursch, R. L. Borup, A. Z. Weber and A. Kusoglu, Effect of Hygrothermal Ageing on PFSA ionomers' Structure/Property Relationship, *ECS Trans.*, 2015, **69**, 1017–1025.

55 F. M. Collette, F. Thominette, S. Escribano, A. Ravachol, A. Morin and G. Gebel, Fuel cell rejuvenation of hygrothermally aged Nafion (R), *J. Power Sources*, 2012, **202**, 126–133, DOI: 10.1016/j.jpowsour.2011.10.135.

56 G. Xie and T. Okada, Fourier transform infrared spectroscopy study of fully hydrated Nafion membranes of various cation forms, *Z Phys. Chem.*, 1998, **205**, 113–125, DOI: 10.1524/zpch.1998.205.Part_1.113.

57 J. Peng, K. Lou, G. Goenaga and T. Zawodzinski, Transport Properties of Perfluorosulfonate Membranes Ion Exchanged with Cations, *ACS Appl. Mater. Interfaces*, 2018, **10**(44), 38418–38430, DOI: 10.1021/acsami.8b12403.

58 G. Xie and T. Okada, The state of water in Nafion 117 of various cation forms, *Denki Kagaku*, 1996, **64**(6), 718–726, DOI: 10.5796/kogyobutsurikagaku.64.718.

59 S. Quezado, J. C. T. Kwak and M. Falk, An Infrared Study of Water-Ion Interactions in Perfluorosulfonate (Nafion) Membranes, *Can. J. Chem.*, 1984, **62**(5), 958–966, DOI: 10.1139/v84-158.

60 M. Falk, An Infrared Study of Water in Perfluorosulfonate (Nafion) Membranes, *Can. J. Chem.*, 1980, **58**(14), 1495–1501, DOI: 10.1139/v80-237.

61 D. E. Moilanen, I. R. Piletic and M. D. Fayer, Water dynamics in nafion fuel cell membranes: The effects of confinement and structural changes on the hydrogen bond network, *J. Phys. Chem. C*, 2007, **111**(25), 8884–8891, DOI: 10.1021/jp067460k.

62 S. A. Roget, P. L. Kramer, J. E. Thomaz and M. D. Fayer, Bulk-like and Interfacial Water Dynamics in Nafion Fuel Cell Membranes Investigated with Ultrafast Nonlinear IR Spectroscopy, *J. Phys. Chem. B*, 2019, **123**(44), 9408–9417, DOI: 10.1021/acs.jpcb.9b07592.

63 J. Kabrane and A. J. A. Aquino, Electronic Structure and Vibrational Mode Study of Nafion Membrane Interfacial Water Interactions, *J. Phys. Chem. A*, 2015, **119**(9), 1754–1764, DOI: 10.1021/jp5084339.

64 R. Basnayake, W. Wever and C. Korzeniewski, Hydration of freestanding Nafion membrane in proton and sodium ion exchanged forms probed by infrared spectroscopy, *Electrochim. Acta*, 2007, **53**, 1259–1264.

65 S. Liu, A. J. A. Aquino and C. Korzeniewski, Water-Ionomer Interfacial Interactions Investigated by Infrared Spectroscopy and Computational Methods, *Langmuir*, 2013, **29**(45), 13890–13897, DOI: 10.1021/la402497w.

66 J. R. Han, N. N. Song, X. Tian, X. L. Zhen and S. X. Liu, Synthesis and structure analysis of sandwich complexes of potassium and cesium with benzo-15-crown-5 derivatives, *J. Inclusion Phenom. Macrocyclic Chem.*, 2013, **77**(1–4), 301–308, DOI: 10.1007/s10847-012-0247-0.

67 D. W. M. Hofmann, L. Kuleshova, B. D'Aguanno, V. Di Noto, E. Negro, F. Conti and M. Vittadello, Investigation of Water Structure in Nafion Membranes by Infrared Spectroscopy and Molecular Dynamics Simulation, *J. Phys. Chem. B*, 2009, **113**(3), 632–639, DOI: 10.1021/jp806761h.

68 M. Laporta, M. Pegoraro and L. Zanderighi, Perfluorosulfonated membrane (Nafion): FT-IR study of the state of water with increasing humidity, *Phys. Chem. Chem. Phys.*, 1999, **1**, 4619–4628.

69 X. Ren, E. Gobrogge and F. L. Beyer, States of water in recast Nafion® films, *J. Membr. Sci.*, 2021, **637**, 119645, DOI: 10.1016/j.memsci.2021.119645.

70 H. Noguchi, K. Taneda, H. Minowa, H. Naohara and K. Uosaki, Humidity-Dependent Structure of Surface Water on Perfluorosulfonated Ionomer Thin Film Studied by Sum Frequency Generation Spectroscopy, *J. Phys. Chem. C*, 2010, **114**(9), 3958–3961, DOI: 10.1021/jp907194k.

71 G. Suresh, Y. M. Scindia, A. K. Pandey and A. Goswami, Self-diffusion coefficient of water in Nafion-117 membrane with different monovalent counterions: a radiotracer study, *J. Membr. Sci.*, 2005, **250**(1–2), 39–45, DOI: 10.1016/j.memsci.2004.10.013.

72 A. Goswami, A. Acharya and A. K. Pandey, Study of self-diffusion of monovalent and divalent cations in Nafion-117 ion-exchange membrane, *J. Phys. Chem. B*, 2001, **105**(38), 9196–9201, DOI: 10.1021/jp010529y.

73 W. Y. Hsu and T. D. Gierke, Elastic Theory for Ionic Clustering in Perfluorinated Ionomers, *Macromolecules*, 1982, **15**(1), 101–105, DOI: 10.1021/ma00229a020.

74 M. Ludvigsson, J. Lindgren and J. Tegenfeldt, FTIR study of water in cast Nafion films, *Electrochim. Acta*, 2000, **45**(14), 2267–2271, DOI: 10.1016/S0013-4686(99)00438-7.

75 S. J. Paddison, The modeling of molecular structure and ion transport in sulfonic acid based ionomer membranes, *J. New Mater. Electrochem. Syst.*, 2001, **4**(4), 197–207.

76 Y. K. Choe, E. Tsuchida, T. Ikeshoji, A. Ohira and K. Kidena, An Ab Initio Modeling Study on a Modeled Hydrated Polymer Electrolyte Membrane, Sulfonated Polyethersulfone (SPES), *J. Phys. Chem. B*, 2010, **114**(7), 2411–2421, DOI: 10.1021/jp906757s.

77 X. Ling, M. Bonn, K. F. Domke and S. H. Parekh, Correlated interfacial water transport and proton conductivity in perfluorosulfonic acid membranes, *Proc. Natl. Acad. Sci. U. S. A.*, 2019, **116**, 8715–8720.

78 Z. X. Liang, W. M. Chen, J. G. Liu, S. L. Wang, Z. H. Zhou, W. Z. Li, G. Q. Sun and Q. Xin, FT-IR study of the microstructure of Nafion((R)) membrane, *J. Membr. Sci.*, 2004, **233**(1–2), 39–44, DOI: 10.1016/j.memsci.2003.12.008.

